Planetary and Space Science 59 (2011) 1681–1694

Contents lists available at ScienceDirect

Planetary and Space Science

journal homepage: www.elsevier.com/locate/pss

New views of the lunar plasma environment

J.S. Halekas [a,d,*], Y. Saito [b], G.T. Delory [a,d], W.M. Farrell [c,d]

[a] Space Sciences Laboratory, 7 Gauss Way, University of California, Berkeley, CA 94720, USA
[b] Institute of Space and Astronautical Science, Japan Aerospace Exploration Agency, 3-1-1 Yoshinodai, Chuo-ku, Sagamihara, Kanagawa 252-5210, Japan
[c] NASA Goddard Space Flight Center, Greenbelt, MD 20771, USA
[d] NASA's Lunar Science Institute, NASA Ames Research Center, Moffett Field, CA 94035, USA

ARTICLE INFO

Article history:
Received 19 May 2010
Received in revised form
9 August 2010
Accepted 11 August 2010
Available online 14 August 2010

Keywords:
Moon
Plasma

ABSTRACT

A rich set of new measurements has greatly expanded our understanding of the Moon–plasma interaction over the last sixteen years, and helped demonstrate the fundamentally kinetic nature of many aspects thereof. Photon and charged particle impacts act to charge the lunar surface, forming thin Debye-scale plasma sheaths above both sunlit and shadowed hemispheres. These impacts also produce photoelectrons and secondary electrons from the surface, as well as ions from the surface and exosphere, all of which in turn feed back into the plasma environment. The solar wind interacts with sub-ion-inertial-scale crustal magnetic fields to form what may be the smallest magnetospheres in the solar system. Proton gyro-motion, solar wind pickup of protons scattered from the dayside surface, and plasma expansion into vacuum each affect the dynamics and structure of different portions of the lunar plasma wake. The Moon provides us with a basic plasma physics laboratory for the study of fundamental processes, some of which we cannot easily observe elsewhere. At the same time, the Moon provides us with a test bed for the study of processes that also operate at many other solar system bodies. We have learned much about the Moon–plasma interaction, with implications for other space and planetary environments. However, many fundamental problems remain unsolved, including the details of the coupling between various parts of the plasma environment, as well as between plasma and the surface, neutral exosphere, and dust. In this paper, we describe our current understanding of the lunar plasma environment, including illustrative new results from Lunar Prospector and Kaguya, and outstanding unsolved problems.

1. Introduction

The lunar plasma environment contains a veritable host of fascinating plasma physics. Despite the seeming simplicity of the lunar environment, the physics of the Moon–plasma interaction has proven complex and varied. Many of the physical processes important in the lunar environment have a fundamentally kinetic nature, primarily because of the small scale of the interaction regions – for example, the plasma interface with sub-ion-inertial-length crustal magnetic anomalies and thin Debye-scale double layers above the charged lunar surface. Given the large gyro-scales for both gyrating solar wind ions and pickup ions, the Moon itself proves small enough to generate very important kinetic effects, especially in the near vacuum of the lunar wake. Furthermore, we find that the Moon acts a natural generator of plasma instabilities, given the host of processes (surface reflection/scattering, secondary and photoelectron emission, ambipolar acceleration, etc.) that produce unstable distributions and counter-streaming beams of both electrons and ions.

The processes described above are fascinating and worthy of study in their own right. In addition to satisfying our intrinsic curiosity, though, we study the Moon as a fundamental plasma physics laboratory with applicability to many other environments and solar system locations. The Moon provides a natural place to investigate basic physics processes such as plasma interaction with surfaces and small-scale magnetic fields, and plasma instabilities, some of which we cannot easily observe elsewhere. At the same time, the Moon provides a place to research many fundamental processes, including ion pickup, sputtering, surface charging, and wake formation, that take place at many other planets, moons, and smaller objects in this solar system.

Scientific study of the lunar plasma environment dates back to the early days of space exploration. Luna 2 made the first space measurements relevant to lunar plasma in 1959 (Dolginov et al., 1960), providing magnetometer evidence that the Moon, unlike the Earth and many other planets, lacked a strong dipolar magnetic field. Beginning eight years later in 1967, and extending over a five-year period, the Explorer and Apollo missions provided data that form the foundation of our understanding of the lunar

* Corresponding author at: Space Sciences Laboratory, 7 Gauss Way, University of California, Berkeley, CA 94720, USA. Tel.: +1 510 643 4310; fax: +1 510 643 8302.
E-mail address: jazzman@ssl.berkeley.edu (J.S. Halekas).

0032-0633/$ - see front matter © 2010 Elsevier Ltd. All rights reserved.
doi:10.1016/j.pss.2010.08.011

plasma environment (see Schubert and Lichtenstein (1974) and Ness (1972) for thorough reviews of these observations). These missions revealed a Moon that has no significant global magnetic field (Sonett et al., 1967; Russell et al., 1978; Dyal et al., 1974) though it does have extensive regions of weak remanent crustal magnetization (Coleman et al., 1972; Anderson et al., 1975). The Moon also has no significant atmosphere (Hoffman et al., 1973), though it does have a weak surface boundary exosphere (Stern, 1999). To first order, one expects absorption of the solar wind plasma at the lunar surface, leading to the formation of a plasma wake behind the Moon (Colburn et al., 1967; Ness et al., 1967). The interplanetary magnetic field (IMF), meanwhile, passes through most parts of the Moon largely unimpeded, with only a small inductive interaction with the conductive lunar interior (Sonett, 1982). Regions of crustal magnetism, though, produce a surprisingly strong solar wind interaction, leading to the formation of limb shocks and or compressions (Ness et al., 1968; Colburn et al., 1971; Russell and Lichtenstein, 1975). Downstream from the Moon, meanwhile, a system of diamagnetic currents forms, producing a characteristic reduction in field strength in the expansion region at the wake boundary, and an increase in field strength in the plasma void (Ness et al., 1968; Colburn et al., 1967, 1971). Schubert and Lichtenstein (1974) described a somewhat different interaction, lacking a clear wake signature, when the Moon passed through the Earth's magnetosphere.

The next significant advance in our understanding of the lunar plasma environment did not come until the Wind spacecraft performed its lunar swing-by maneuvers, in 1994 (Ogilvie et al., 1996; Owen et al., 1996; Farrell et al., 1996). Since that date, the number of missions making relevant measurements has exploded, with many spacecraft, launched by many countries, contributing to a new and refined understanding of the lunar plasma interaction. Geotail, Wind, Lunar Prospector Nozomi, Kaguya, Chang'E, and Chandrayaan in particular have contributed to this renaissance. In this paper, we detail the advances in lunar plasma science over the last sixteen years, with a particular emphasis on describing the many aspects of the Moon–plasma interaction that a purely magnetohydrodynamic picture cannot account for. We also include illustrative data from Lunar Prospector (LP) and Kaguya and discuss future directions.

2. Global moon–plasma interaction

2.1. Dayside interaction

The Moon's surface, not protected by any significant atmosphere or global magnetic field, sits directly exposed to the surrounding solar wind and/or magnetospheric plasma, and to solar photons and solar energetic particles as well. Not surprisingly, solar influences strongly drive the global Moon–plasma interaction, affecting the plasma environment directly, and also influencing the surface and exosphere and their respective interfaces with the plasma. Fig. 1 shows an overview of some of the major plasma processes in the lunar environment.

To first order, the solar wind interacts relatively weakly with the dayside lunar surface, with most ions impacting and implanting into the surface. Relatively few manifestations of the interaction propagate back upstream from the Moon, especially in regions with no remanent crustal magnetism. Even above crustal fields, few phenomena have proven measurable more than a few hundred kilometers upstream from the lunar surface. Recent observations, though, have shown that ion scattering/reflection form a more important part of the dayside lunar surface interaction than previously thought, suggesting that some lunar effects may indeed propagate upstream from the surface. Thanks to observations from Kaguya, Chandrayaan, and IBEX, we now know that ~10–20% of solar wind ions reflect from the surface, with 0.1–1% of them remaining charged (Saito et al., 2008; Holmström et al., in press), and the remainder gaining an electron to become energetic neutral atoms (ENAs) (Wieser et al., 2009; McComas et al., 2009). Neutral hydrogen atoms have a long lifetime against photoionization and should not strongly interact with the lunar environment, but the reflected protons may have interesting consequences, given their large relative velocity with respect to the solar wind population and the resulting potential for instability formation (Holmström et al., in press). In addition, these reflected protons feel the force of the convective electric field and the IMF and follow cycloidal pickup ion trajectories, seen by Kaguya as self-pickup accelerated ions (Saito et al., 2008), and possibly also observed by Nozomi (Futaana et al., 2003). Some of these re-picked up solar wind ions re-impact the surface, while

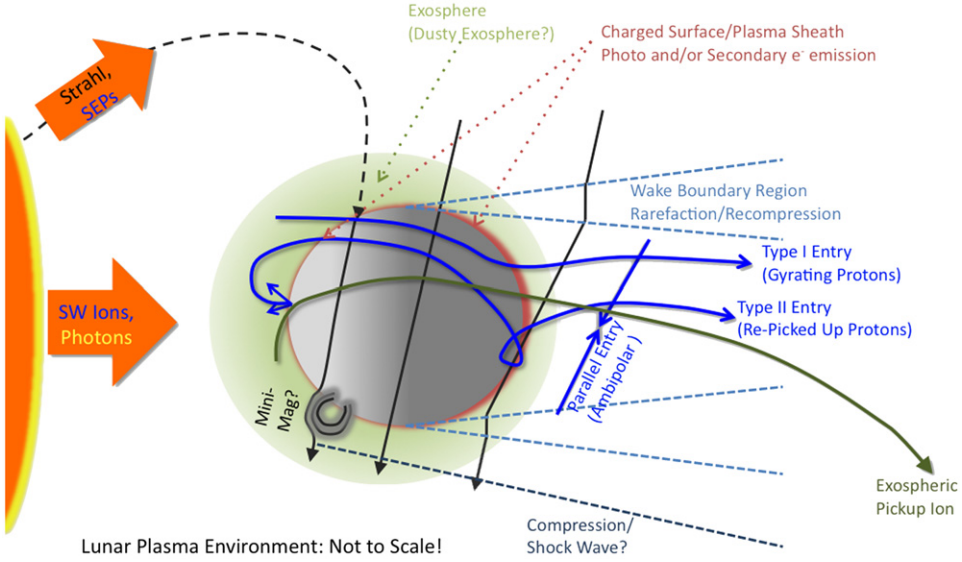

Fig. 1. Overview of solar drivers and fundamental physical processes in the lunar plasma environment, including solar wind scattering, pickup processes, wake formation and refilling, crustal magnetic field interactions, and surface charging.

others escape and propagate downstream. For some launch points and solar wind conditions, these re-picked up solar wind ions have gyro-orbits such that they can enter the tenuous lunar wake (Nishino et al., 2009b) (as shown in Fig. 1), where they can have strong, even dominant, effects on the tenuous local plasma (Nishino et al., 2009b, in press) (as described further in Section 2.2).

In addition to reflected solar wind protons, sputtering from the lunar surface (Elphic et al., 1991) and ionization of the neutral exosphere can produce heavier pickup ions, previously observed far downstream (tens of thousands of km or more) from the Moon by several spacecraft (Cladis et al., 1994; Hilchenbach et al., 1993; Mall et al., 1998), and more recently at ~100 km altitude by Kaguya (Yokota et al., 2009). Therefore, the Moon provides not only a sink, but also a source, of plasma in the solar wind. This source of plasma has rather low flux compared to the solar wind, but could nonetheless still produce significant and observable effects around the Moon, given the very different composition and 3-d velocity distribution of these ions compared to the dominant solar wind flux. These ions, similarly to the re-picked up solar wind protons, may re-enter the plasma wake cavity further downstream in their cycloidal gyration, as shown in Fig. 1, locally introducing significant perturbations to the wake structure and dynamics. In addition, measurement of these pickup ions can provide information about the composition of the surface and exosphere, as well as the dynamics of the respective plasma interaction regions, as described by Yokota and Saito (2005) and Hartle and Killen (2006).

2.2. Lunar plasma wake

The Moon apparently does not strongly affect the environment upstream from it, acting only as a source of rather tenuous neutral atoms as well as ions produced via photoemission, impact ionization, and charge exchange. However, significant influences on the surrounding plasma unquestionably propagate to large distances downstream, as Wind observations of the lunar wake at up to 25 R_L (~43,000 km) (Clack et al., 2004) show. The lunar wake forms because of the removal of solar wind ions and electrons at the dayside, through both absorption/implantation and scattering/reflection, resulting in a nearly complete plasma void immediately downstream from the nightside hemisphere of the Moon. As the supersonic solar wind flows past the Moon, solar wind plasma refills this void region, with many interesting consequences.

The wake cavity region typically has moderately enhanced fields compared to the solar wind, while the "expansion region" immediately surrounding the wake has correspondingly reduced fields (Ness et al., 1968; Colburn et al., 1967, 1971). These magnetic field perturbations, which correspond to changes in the field direction as well as magnitude (as seen in Fig. 1), result from a diamagnetic current system produced by the pressure gradient across the wake boundary (Colburn et al., 1967; Owen et al., 1996). Equivalently, one can think of these effects on the magnetic field in terms of plasma expansion and recompression, assuming the frozen-in condition (Whang, 1968a, 1968b; Johnson and Midgeley, 1968; Michel, 1968). The expansion region corresponds to a rarefaction region, bounded externally by a rarefaction wave, and the central wake to a recompression region, as shown in Fig. 1. Finally, many spacecraft have observed additional external magnetic enhancements, clearly correlated in location with crustal magnetic sources, variously termed "limb shocks", "limb compressions", and "Lunar External Magnetic Enhancements", outside of the wake and expansion regions (Ness et al., 1968; Colburn et al., 1971; Russell and Lichtenstein, 1975; Lin et al., 1998; Halekas et al., 2006a, 2008b). We will discuss these last features, also shown in Fig. 1, in more detail in Section 4.

The wake has a number of modes of particle entry, many of which have only recently been observed and properly appreciated. In a fluid picture, one would expect that plasma should refill the wake via a magnetosonic wave mode, and the first models of the wake indeed assumed this, with some predictions treating the wake boundary as a tangential discontinuity with no cross-boundary flow, forming a trailing shock wave at the downstream convergence of the refilling plasma (Spreiter et al., 1970). According to most fluid models, the wake should fill in an asymmetric fashion, with the asymmetry determined by the magnetoacoustic velocity anisotropy. Whang and Ness (1970) found that the rarefaction wave approximately obeyed such a relation, but Sonett and Mihalov (1972) found that the external enhancements followed a relationship seemingly inconsistent with magnetosonic expansion, given a large inferred velocity anisotropy inconsistent with typical solar wind conditions. However, both of these investigations relied on features without a natural cylindrical symmetry, making such a determination difficult at best. Halekas et al. (2005b) later attempted to use electron data to determine the refilling mode at low altitudes, and successfully ruled out a purely static magnetic field with particle entry along field lines, but could not rule out either purely cylindrically symmetric ion sonic expansion or magnetosonic expansion based only on electron measurements (though magnetic field data seemingly rule out purely symmetric ion sonic expansion). Recent ion observations conclusively rule out any treatment of wake refilling via a purely magnetosonic or sonic wave mode, at least at low altitudes. Instead, a complete description of wake refilling must take into account a number of kinetic effects.

Far downstream from the Moon ($> 6.6\ R_L$), Wind observations indicate ion refilling primarily along magnetic field lines. This process unfolds with more mobile electrons leading the expansion into the wake, resulting in a charge separation electric field and a potential drop across the wake boundary that both slows the electron expansion and accelerates ions along field lines into the wake (as shown in Fig. 1) at a velocity related to the ion sound speed (Ogilvie et al., 1996). The resulting beam of cold ions can have large temperature anisotropies (Clack et al., 2004), and beams from the two sides of the wake can meet and interpenetrate in the center of the wake, possibly leading to instabilities (Farrell et al., 1998). Meanwhile, the wake potential excludes some electrons from the wake, resulting in a cutoff energy of electrons that can pass through the wake – the resulting filtered electron distribution may stimulate whistler turbulence observed outside of the wake (Nakagawa et al., 2003). The excluded low energy electrons, meanwhile, will reflect from the potential, producing a counter-streaming distribution that could also excite waves (Futaana et al., 2001; Farrell et al., 1996). Differential shadowing of electrons and ions may generate further current systems and instabilities (Bale et al., 1997). The wake potential may also result in pitch angle diffusion of particles near the wake boundary (Nakagawa and Iizima, 2006).

The ambipolar expansion process has been described theoretically (Samir et al., 1983), and modeled extensively, both from the general standpoint of plasma expansion into a void (Crow et al., 1975; Denavit, 1979) and from a specifically lunar viewpoint (Farrell et al., 1998, 2008a; Birch and Chapman, 2001a, 2001b; Kallio, 2005; Trávnicek and Hellinger, 2005; Kimura and Nakagawa, 2008), with great success. Halekas et al. (2005b) extended the basic theory of ambipolar wake expansion to take into account the energetic tail of the solar wind electron distribution, thereby explaining an increase in electron temperature observed in the wake by LP (Halekas et al., 2005b) and Wind

(Ogilvie et al., 1996) in terms of velocity filtration of a non-Maxwellian distribution of solar wind electrons.

The degree to which quasi-neutrality holds in the wake remains under debate. Quasi-neutrality usually provides a very close approximation of space plasma processes, and most theoretical descriptions of the wake expansion assume perfect quasi-neutrality, but some simulations (Crow et al., 1975; Farrell et al., 2008a) indicate an "expansion front", where an electron cloud precedes the ions into the wake. If this picture proves correct, it has fascinating implications for charging and discharging of the surface and objects on the surface in the wake, as this electron cloud could drive the surface to unexpectedly large negative potentials, especially if no mitigating current exists (Farrell et al., 2008a, 2008b, 2010).

Closer to the Moon, absent ion observations, researchers assumed that a similar expansion process operated. However, Kaguya and Chang'E have now shown that, while ions do enter the wake parallel to field lines at low altitudes, they also enter the wake perpendicular to field lines close to the Moon. At least two processes lead to wake entry perpendicular to the field lines. First, the finite temperature of solar wind ions ensures that they gyrate in the solar wind frame. This gyration allows some ions to enter the wake perpendicular to magnetic field lines. Fig. 1 shows this process, termed Type-I entry (Nishino et al., 2009a). Intriguingly, as these gyrating ions enter the wake, they apparently feel the effects of a potential drop and experience an E X B drift parallel/anti-parallel to the solar wind flow near the wake boundary, resulting in energy gain/loss in the Moon frame as they enter from the two flanks of the wake (Nishino et al., 2009a). The pair-wise energy gain/loss features therefore seemingly indicate that ambipolar processes may also operate at low altitudes near the Moon, consistent with electron observations (Halekas et al., 2005b). However the angular dependence of the ambipolar potential remains poorly understood. Most expansion models predict an electric field exactly parallel to magnetic field lines, but the observations of Type-I entry suggest the presence of a component of the electric field perpendicular to the magnetic field.

Scattered ions, re-picked up in the solar wind, provide another source of ion entry perpendicular to the magnetic field line – so-called Type-II entry (Nishino et al., 2009b), also shown in Fig. 1. This entry process allows ions to enter deep into the plasma void, with a flux apparently significant enough to provide a significant perturbation to the charge density in the wake. This supplemental charge density proves large enough to accelerate electron beams into the wake (Nishino et al., 2009b), generating significant electrostatic turbulence (Nishino et al., in press). In this case the ions pull the electrons into the wake, opposite to the usual ambipolar expansion along field lines. This process produces anomalous bursts of electrons along field lines in the deep wake, observed by both Kaguya and LP. Most recently, Chang'E observations have shown that these scattered and re-picked up solar wind ions sometimes also feel the effects of a potential drop, experiencing additional acceleration into the wake as they enter the cavity perpendicular to field lines (Wang et al., 2010). Again, this implies the existence of a perpendicular component of the ambipolar electric field near the Moon.

2.3. Future directions

Many of the processes described in this section can and do operate simultaneously in the lunar plasma environment, as shown by an illustrative orbit of Kaguya MAP-PACE data, in Fig. 2. This figure shows many of the processes discussed above, all on one orbit, cutting through the wake at one altitude, at a limited range of local time, in a plane roughly perpendicular to the plane

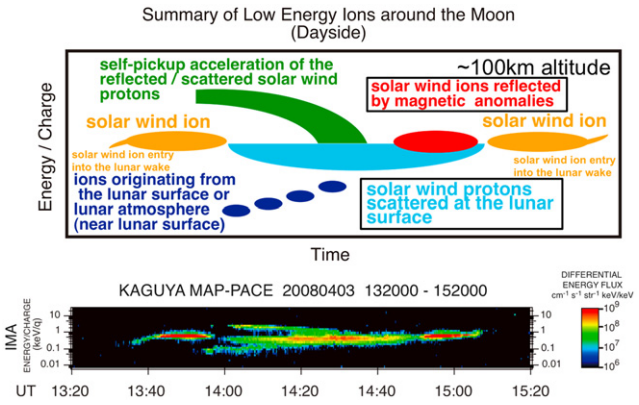

Fig. 2. Overview of ion processes observed by Kaguya, including exospheric pickup ions, solar wind scattering, re-picked up solar wind ions, reflection from magnetic anomalies, and wake entry. Top panel identifies components in data (with expanded vertical axis).

of the magnetic field. The Kaguya data on this orbit show ion scattering and re-pickup from the dayside, pickup ions from the exosphere and/or surface, magnetic anomaly interaction, and Type-I entry at the wake flanks. At the same time, at other regions around the Moon (as shown schematically in Fig. 1), ambipolar ion entry should take place parallel to the magnetic field lines, Type-II entry may take place in some regions of the wake, and pickup ions from the exosphere and/or surface may re-enter the wake far downstream. All of these processes have a fundamentally kinetic nature, and the interplay between them will no doubt prove difficult to untangle. In addition, the work of describing the Moon–plasma interaction when it passes through the Earth's magnetotail, an entirely different plasma regime, has just begun (Tanaka et al., 2009). The two-spacecraft constellation ARTEMIS (Angelopoulos et al., 2010) will soon arrive in orbit around the Moon, and its comprehensive instrumentation, two-probe measurement technique, and comprehensive orbital coverage, should lead to further advances in our understanding of the extended global Moon–plasma interaction region.

3. Surface–plasma interaction

3.1. Surface charging

The lunar surface, like any object immersed in plasma, charges to an electrostatic potential. This potential, assuming equilibrium (a good assumption for the Moon, given typical charging time scales $\ll 1$ s), develops such that all the currents to the surface balance. This current balance, for a purely conductive body, should hold globally. The Moon, however, has low enough surface conductivity (Schwerer et al., 1974), especially at night (Alvarez, 1977), that this current balance need only hold locally. Thus, each portion of the lunar surface charges in order to balance all currents to it, including plasma currents from electrons and ions, photoelectron currents generated by solar photons, and secondary electron emission from both electron and ion impact (see Whipple (1981) for a thorough review of charging processes). In sunlight, photoemission should generally provide the largest current source, and the surface should charge to positive potentials on the order of the photoelectron temperature (a few eV), sufficient to return most photoelectrons to the surface. In shadow, on the other hand, electron thermal flux dominates, and the surface should generally charge negative to values on the order of the electron temperature, unless secondary emission proves significant. Theoretically, given high enough secondary emission

efficiency, the nightside surface could charge positive, but few observations to date support this possibility at the Moon, though the ~100 eV electron temperature often observed in the wake could lead to increased secondary emission. A non-neutral plasma sheath (double layer) forms above the charged surface, with a scale height roughly related to the Debye length of the dominant current carrier. This layer effectively shields the charged surface from the surrounding plasma, ensuring that surface charging generally does not directly affect the surrounding environment at high altitudes above the sheath. However, charged particles accelerated from these surfaces certainly can and do affect the lunar environment.

The Apollo SIDE surface experiment suggested a lunar surface potential that, commensurate with expectations, generally equilibrates at small positive values in the solar wind on the dayside at small solar zenith angles (SZA) (Fenner et al., 1973; Freeman et al., 1973; Freeman and Ibrahim, 1975), with potentials decreasing as a function of SZA and going negative some tens of degrees before the terminator due to the reduction in photoelectron and solar wind ion flux at glancing incidence, and reaching −50 to −100 V near the terminator (Freeman et al., 1972; Lindeman et al., 1973; Benson, 1977). The SIDE potential measurement techniques had limited utility in shadow, and therefore provided few constraints on nightside surface charging.

More recently, the LP mission pioneered the measurement of negative surface potentials, providing a better understanding of surface charging on the lunar night side. As first shown by Halekas et al. (2002), one can extract information about the potential drop between the spacecraft and the surface by measuring the electron distribution above the surface and identifying boundaries in phase space between incident electrons, magnetically and electrostatically reflected electrons, empty regions of phase space formed by electron loss to the surface (the "loss cone"), and secondary electrons accelerated up from the lunar surface. The key observations indicative of negative surface charging below the spacecraft are energy-dependent loss cones, with measurements at a range of energies thereby allowing separation of electrostatic and magnetic reflection effects, and beams of secondary electrons accelerated upward from the surface through the potential drop.

Unfortunately, the electron reflectometry technique only provides the potential drop between the spacecraft and the surface, and spacecraft charging proves troublesome and difficult to correct for (Halekas et al., 2008c, 2009b). In addition, in the wake, one will in general measure a component of the ambipolar field across the wake (see Section 2.2), in addition to the potential drop at the surface (Halekas et al., 2008c). Finally, finite gyroradius effects lead to underestimated potential drops when magnetic field lines intersect the surface at oblique angles, since an electron on a tilted field line that reflects just before reaching the surface (thereby defining the loss cone boundary) senses a smaller gyro-averaged potential than a corresponding electron on a field line normal to the surface (Halekas et al., 2003). It is now possible to apply corrections for the effects of these issues, by using a spacecraft charging model developed for LP (Halekas et al., 2008c), utilizing a self-similar model of low-altitude ambipolar potential in the wake (Halekas et al., 2005b), and applying an empirical ad hoc correction for the tip angle effect (Halekas et al., 2003). All of these corrections have been applied to produce the first global map of average lunar surface potential in the solar wind and wake (relative to the local plasma just above the sheath), shown in Fig. 3.

The global map (Fig. 3) indicates that the surface at SZA < ~60° has either a positive potential or a small negative potential. The available data cannot rule out a negative dayside surface potential, though a small positive potential conforms

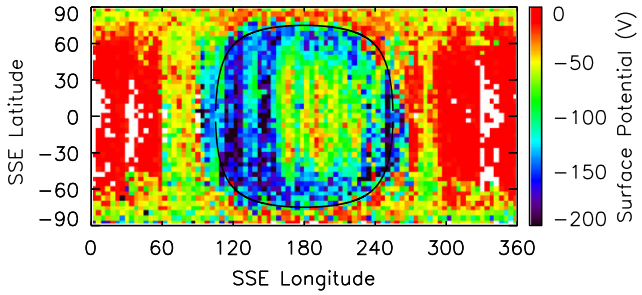

Fig. 3. Median electrostatic potential of the lunar surface in the solar wind, in spherical Selenocentric Solar Ecliptic coordinates, relative to the local plasma. Black line indicates the average wake boundary at spacecraft altitude.

more closely to previous observations and theoretical expectations (Singer and Walker, 1962; Manka, 1973; Stubbs et al., 2007b) (see more discussion in Section 3.4). Given the limited low energy coverage of the LP instrumentation, we cannot easily resolve this question observationally. However, the surface potential unquestionably starts to go significantly negative (~−50 V average) at SZA of ~60–70°, again in rough accord with expectations from theory and previous measurements (Stubbs et al., 2007b; Benson, 1977). In full shadow, past SZA of 90°, the surface potential drops steeply, reaching its most negative values relative to the local plasma of ~−100 to −200 V. At the largest SZA (greater than ~135°) the magnitude of the negative surface potential surprisingly decreases. This reduction in negative potential may result from increased secondary electron emission induced by the greatly enhanced electron temperature in the central wake (Halekas et al., 2008c). We must emphasize that Fig. 3 shows the surface potential relative to the local wake plasma, not relative to the solar wind outside the wake. Given the effects of the large potential drop into the wake, the surface potential relative to the undisturbed solar wind should remain at or close to its maximum negative value of ~−400 V in the center of the wake. We note the presence of some potential variations not related to solar zenith angle, for instance larger negative potentials at longitudes of 120–150° than at 210–240°. These may result from geographic variations and/or from the dominant Parker spiral IMF orientation, which will affect electron access to the lunar night side.

The general picture of surface charging in the Earth's magnetotail remains similar to that in the solar wind, but with some important differences. First, in the magnetotail, with no solar wind flow and therefore no wake, the primary day/night differences result from the presence/absence of photoemission. The plasma input to the night side remains nearly constant over the entire shadowed hemisphere, resulting in a commensurate lack of spatial variation in the nightside potential. However, the temporal variability of the surface charging, if anything, increases, due to the many rapid transitions between tail lobe and plasmasheet observed at lunar orbit. The plasma properties in both of these very different regions have interesting consequences for surface charging. In the very tenuous tail lobe regions, it appears that the surface potential may at times reach very large positive values (since few ambient electrons exist to balance escaping photoelectron fluxes) as suggested by both Apollo CPLEE surface observations (Reasoner and Burke, 1972) and more recent Kaguya orbital data (Tanaka et al., 2009). Meanwhile, in the very hot and dynamic plasmasheet, the lunar surface regularly reaches negative surface potentials of up to −2 kV (Halekas et al., 2005a). Intriguingly, we regularly observe these large negative potentials even in sunlight, despite the seeming inability of the observed plasma electron currents to balance the expected photoemission (Halekas et al., 2005a, 2008c). These observations have significant

consequences, suggesting either lower than expected photoemission, or possibly non-monotonic potential structures. We will discuss the latter possibility further in Section 3.4.

3.2. Extreme events

The most significant lunar nightside charging observed to date by LP has taken place during large solar energetic particle (SEP) events, when the typically observed nightside charging level shown in Fig. 3 increases by over an order of magnitude, resulting in negative nightside surface potentials of up to −4 kV (Halekas et al., 2007, 2009b). Energetic particle inputs clearly drive the surface to these extreme potentials, but the exact role of electrons, ions, and secondary electrons remains somewhat unclear (Halekas et al., 2009b).

In Fig. 4, we show a single orbit of LP data during an early phase of an SEP event, during a time period with a very anisotropic (field-aligned) primary electron distribution characteristic of the early portion of many SEP events. We see a number of interesting features in this data, many of which have not been previously explored. Fig. 4 shows a series of energy spectrograms, for five different pitch angle ranges. Absent lunar influences, the bottom-most spectrogram in Fig. 4 (most anti-field-aligned electrons) primarily contains the energetic anisotropic population, while the other spectrograms contain a more diffuse and less anisotropic distribution.

From 17:40 to 17:58 and from 19:16 to 19:40, the incoming anisotropic electron population travels along magnetic field lines connected to the dayside of the Moon, as indicated by the "Pol" color bar in Fig. 4. The non-zero population of electrons coming from the Moon during these time periods (top two spectrograms in Fig. 4) indicates some combination of backscattered electrons, photoelectrons, secondary electrons, magnetically and/or electrostatically reflected primary electrons, electrons that have experienced significant pitch angle diffusion, and/or electrons reflected/accelerated by wave particle interactions. Given the clear disruption of the incoming beam, and the low frequency turbulence observed in the magnetic field, we suspect at least a component of pitch angle diffusion and/or wave–particle interactions; however, the full interaction might include any or all of these effects.

From 17:58 to 18:18 and from 19:02 to 19:16, the magnetic field at the spacecraft, according to a straight-line trace, does not connect to the Moon. During the later time period (exit side of wake), the magnetic field does not intersect the lunar surface or the wake, and we observe few lunar influences on the electron distribution, as expected – thus, this period shows something like

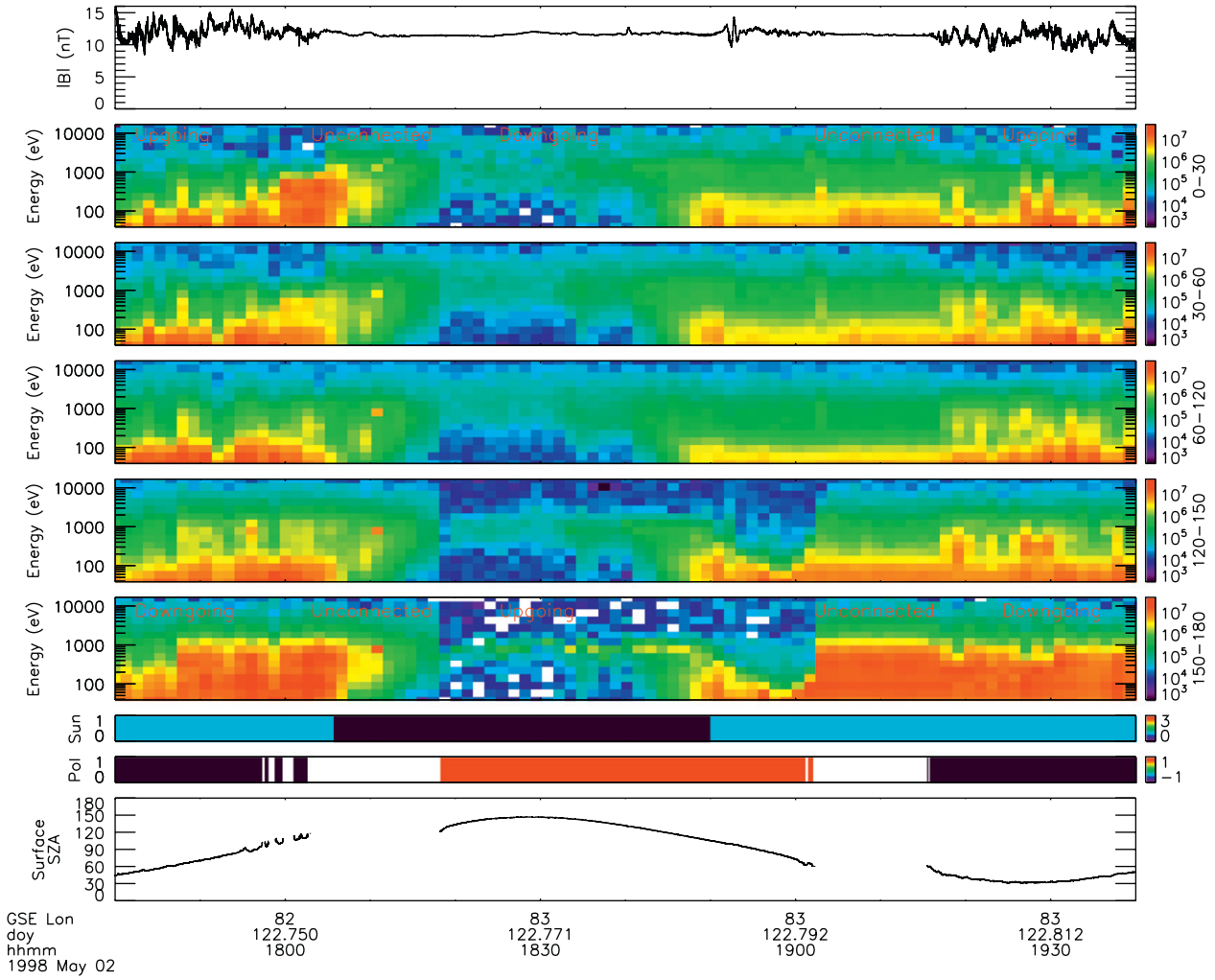

Fig. 4. Lunar Prospector orbit in the solar wind during the early stages of a solar energetic particle injection on May 2 1998, showing magnetic field magnitude, electron differential energy flux (eV/(cm^2 sr s eV)) in five different pitch angle channels (0–30, 30–60, 60–120, 120–150, 150–180), sun/shadow color bar "Sun" (blue=sun, black=shadow), magnetic connection to surface "Pol" (assuming no field curvature, red=positive connection, black=negative connection, white=no connection), and solar zenith angle of connection to surface. (For interpretation of the references to color in this figure legend, the reader is referred to the web version of this article.)

the unperturbed upstream electron input. Meanwhile, during the earlier time period (entry side of wake), the field lines point into the wake, and the ambipolar wake potential reflects most of the incident electron population. As the spacecraft travels into the wake during this time period, the potential drop traversed by the measured primary electrons increases, reflecting more and more of the incident population, and leaving only a hotter and more tenuous filtered population in the wake.

Finally, from 18:18 to 19:02, the Moon blocks the main electron population (note that the region that this energetic electron population cannot access is not exactly the same as the plasma wake, since the wake is controlled by the solar wind ion flow and corresponds more closely to the light/shadow boundary seen in the "Sun" color bar), leaving only a more diffuse upstream-propagating population to impact the lunar night side. The wake potential also filters this residual population, leaving a very hot and tenuous incident electron population in the central lunar wake. This population drives the surface potential to large negative values, producing a beam of secondary electrons accelerated upwards through the near-surface potential drop to the spacecraft, as clearly seen in the bottom spectrogram of Fig. 4. This beam reaches an energy of $\sim$0.8–1.5 keV (on the order of the temperature of the incident electrons, and with variations corresponding to the variation in that population), indicating a peak negative surface potential of at least ~ -1.5 kV. The beam appears more localized in both energy and angle in the deepest part of the wake (farthest anti-solar region), possibly because of the larger Debye length there, which leaves plasma instabilities fewer Debye lengths in which to alter the beam before it reaches spacecraft altitude. Large upward-going fluxes suggesting negative surface charging persist well into sunlight (up to SZA $\sim$60°), albeit at reduced levels, during the time period from 18:50 to 19:00.

This sample event serves to represent the complexity and detail of the wake structure and surface interaction around the Moon (and the interplay between these two components of the lunar plasma environment). We can clearly anticipate from events like this one that the details of the plasma interaction will generally depend sensitively on the properties of the incident electron distributions and the magnetic geometry of each event. In the following section(3.3) we discuss electron velocity distributions in more detail, using this same event as an example.

3.3. Electron emission from the surface

Given the many sources of upward-traveling electrons discussed in the previous section (3.2), we need to understand both reflected primary electrons and electrons emitted from the surface to understand the lunar plasma environment. Photoelectrons and secondary electrons from the surface provide a particularly useful diagnostic of the surface interaction, since they must pass through any magnetic gradient or potential drop above the surface before reaching the spacecraft. Since photoelectrons and secondary electrons from both electron and ion impact should start with a relatively low characteristic temperature of a few eV (Whipple, 1981), one can often determine many of the characteristics of both the magnetic and electric field configuration below the spacecraft by measuring these surface-generated electrons. Furthermore, beyond their use as a diagnostic, we can predict that these electrons should have a significant effect on the surrounding plasma, though the altitude range to which this influence may extend remains in doubt, since no one has yet observed these surface-emitted electrons more than $\sim$100 km from the Moon. Finally, if we can unambiguously observe a particular population of electrons from the surface, we can put constraints on the physical properties of surface materials, as attempted by Halekas et al. (2009a) for the case of secondary electron emission.

A typical observation of an electron distribution above the lunar night side shows a beam of electrons traveling upward along the magnetic field line from the surface, likely composed of secondary electrons accelerated through the potential drop from the negatively charged surface (Halekas et al., 2002, 2008c). We consider this interpretation of the nightside distributions plausible and physically likely, since the energy of the beam typically corresponds to the potential drop one infers from the energy dependence of the loss cone. However, previous studies may have insufficiently appreciated one major complication to this picture. For parallel magnetic and electric fields, we should indeed expect a beam of electrons; however, for non-parallel magnetic and electric fields, near-surface acceleration through a Debye-scale double layer should in general lead to a gyrating conic distribution of electrons rather than a beam. We do not often observe such a conic distribution above the night side (though beams do often appear more broad in angle than expected), suggesting the presence of some additional focusing mechanism. Small-scale crustal magnetic fields, resulting in a near-surface magnetic gradient and adiabatic focusing, provide one candidate focusing mechanism (though pitch angle scattering and/or wave particle interactions could also prove important). We know from Apollo surface magnetometer measurements that surprisingly strong fields exist at some surface locations (Dyal et al., 1974), even in regions where we only observe relatively weak fields at orbit altitudes. Additionally, a recent study of the electron reflectometry technique shows that neither electron reflectometry nor magnetometer measurements from orbit can reliably detect such fields, as long as they have spatial wavelengths of a few km or less (Halekas et al., 2010) (as observed at the Apollo 16 landing site, for example). Therefore, a significant distribution of small-scale crustal magnetic fields whose influence extends only a few km or less above the surface could act to adiabatically focus secondary electrons, without contradicting any observations to date. Clearly, other possibilities exist, but nothing rules such an effect out. If such magnetic focusing does prove important, we can predict that it would not operate as efficiently on the day side, since the solar wind dynamic pressure will compress most small-scale crustal fields below the surface.

With these considerations in mind, we survey electron distributions observed during the event of Fig. 4, at four different times, in the four panels of Fig. 5. Panel A shows a distribution observed from the spacecraft in sunlight, while briefly connected to the nightside surface near the wake boundary. We find a loss cone consistent with purely electrostatic reflection by a potential drop of $\sim$500 V, as shown by the over-plotted loss cone fit. This reflection may result from a combination of surface potential and wake ambipolar potential drop along the magnetic field line. Outside of the loss cone, the reflected flux is equal to the corresponding incident flux for most portions of the distribution, but we see excess flux at angles of 120–150°, indicating a surplus of upward-going particles. Given the energy of these upward-going electrons of $\sim$500 eV, these electrons could represent a conic of secondary electrons accelerated from the surface, but they could also result from pitch angle scattering of the reflected anisotropic electron distribution, especially given their low absolute flux level compared to the more field-aligned incident and reflected components of the distribution (Fig. 4 shows that field-aligned fluxes greatly exceed more obliquely traveling fluxes at this time).

Panel B of Fig. 5 shows a much more typical nightside observation (with higher noise levels because of the much lower fluxes in the deep wake) with a very clear upward-going beam

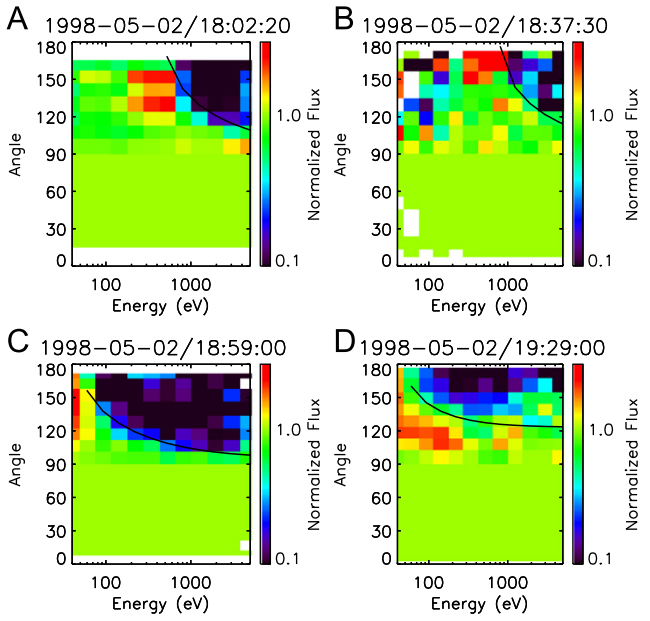

Fig. 5. Four energy/angle spectrograms during the event of Fig. 4. Each distribution shows upward-traveling electrons from 90 to 180, with both halves of the distribution normalized to the downward-going (0 to 90) angular distribution. Regions with normalized flux less than one indicate a deficit of reflected particles (due to loss to the surface), while those with normalized flux greater than one indicate a surplus of reflected particles (likely produced by secondary emission and/or pitch angle scattering and/or wave–particle interactions). We show tentative loss cone fits for potential drops of −500 V (panel A), −800 V (B), −50 V (C), and −50 V (D) for the four distributions.

consistent with the typical interpretation of secondary electrons accelerated along the field line through the potential drop of ~ -800 V.

Panel C of Fig. 5 shows a distribution much like that in the first panel, but indicating a much lower surface potential, consistent with the location of the spacecraft above the dayside, and magnetic connection to a dayside region with SZA of $\sim 60^\circ$ (as compared to the $\sim 120^\circ$ surface location of the first observation). This distribution most plausibly represents a conic of secondary electrons (and/or photoelectrons, given the dayside surface location) accelerated from the surface, given the high excess fluxes of upward-going electrons at an energy corresponding closely to the estimated potential drop of −50 V.

Finally, panel D of Fig. 5 shows a distribution that, though still plausibly fit by an adiabatic loss cone model for a drop of −50 V, does not display the same clear loss cone of the other three distributions. Surrounding the purported loss cone, we observe enhanced upward-going electron flux, extending well above the potential drop suggested by the loss cone fit. Therefore, we cannot explain these electrons purely in terms of accelerated secondary electrons or photoelectrons; instead, they must result from wave–particle interactions and/or pitch angle scattering, as also suggested by the turbulent magnetic field and the disruption of the incident primary electrons at this time (see Fig. 4). Given these considerations, the loss cone in this distribution may or may not indicate the presence of a static negative surface potential. A negative potential would also disagree with theoretical expectations of predominantly positive dayside potentials, given the nearly sub-solar location of this observation.

These electron distributions, particularly those observed in sunlight, again speak to the extreme complexity of the Moon–plasma interaction. Numerous processes, including, but not limited to, adiabatic reflection, secondary acceleration, backscatter, wave–particle interactions, and pitch angle scattering likely operate in the lunar environment, and affect the electron distributions that we observe. In order to truly understand these distributions, we will require both detailed case studies and statistical surveys, with complete plasma instrumentation.

3.4. Future directions

The observations discussed in the preceding sections indicate a complex lunar surface interface that varies dramatically due to temporal changes in the properties of the incident plasma and IMF, and due to spatial variations in incident plasma and solar radiation over the surface of the Moon. For instance, the properties of the wake plasma heavily influence the surface interface; in turn, the surface could affect wake refilling, especially near the terminator.

Indeed, the near-terminator region, including the poles, presents a very interesting environment. The presence of the light/shadow boundary here could lead to significant lateral potential variations over small scales, and thus large electric fields, especially in regions with significant topography (Criswell and De, 1977; De and Criswell, 1977). Local "orographic" mini-wakes extending downstream from topographic features (for instance, polar craters) near the terminator/polar regions could enhance and/or add to these fields, especially if the ambipolar expansion process results in a non-quasi-neutral region with enhanced negative charge, which would in turn charge the surface anomalously negative (Farrell et al., 2010). Dust also charges in a plasma (Horányi, 1996), and electrostatic transport of dust has been achieved in the laboratory (Doe et al., 1994; Sickafoose et al., 2002; Colwell et al., 2009; Wang et al., 2009) and modeled theoretically (Nitter et al., 1998; Nitter and Havnes, 1992; Stubbs et al., 2006, 2007c; Borisov and Mall, 2006). A number of lines of evidence suggest that some process(es) may loft lunar dust above the surface near the terminator regions, at least to a few meters (Rennilson and Criswell, 1974; Berg et al., 1976), but possibly to tens of kilometers or more (McCoy and Criswell, 1974; Zook and McCoy, 1991). Electrostatic forces provide the most plausible explanation for this dust transport; therefore, the details of the lunar plasma interaction near the terminator may significantly affect lunar dust, with possible impacts on exploration (Stubbs et al., 2007a). The proposed LADEE (Lunar Atmosphere and Dust Environment Explorer) mission, especially in concert with ARTEMIS, will hopefully shed more light on this question. However, the best way to understand the polar/terminator environment may be to place a dusty-plasma landed package in the region to examine surface charging, plasma currents, and dust transport.

Another important scientific question relates to the structure of the plasma sheath near the dayside surface. Generally, one assumes a monotonic potential variation from the surface to the ambient plasma. However, theoretical investigations show that a second solution, with a non-monotonic potential variation, can equally well balance currents to the dayside surface (Fu, 1971; Guernsey and Fu, 1970; Nitter et al., 1998). For this solution, a potential well generated by space charge acts to trap more of the photoelectrons near the surface, while also reflecting part of the incoming electron population before it reaches the surface. With such a potential well, the sunlit surface can float to less positive potentials than otherwise possible, even reaching negative potentials relative to the ambient plasma for some conditions. Some questions remain as to the energetic favorability of this solution (Nitter et al., 1998), but the most recent particle-in-cell models (Poppe and Horányi, in review) also converge on a non-monotonic solution for the potential above dayside in the solar wind. This non-monotonic potential structure could have interesting implications, because it allows the dayside surface to float to larger negative values than

otherwise possible – potentially allowing us to explain the large negative dayside surface potentials observed in the plasmasheet (Halekas et al., 2005a, 2008c) without requiring a lower than expected photoemission efficiency from the surface. In addition, the small negative potentials often measured on the lunar dayside in the solar wind (Halekas et al., 2008c) might also prove real, rather than representing erroneous measurements of potentials below the noise level of the reflectometry technique, as previously assumed. ARTEMIS, with its comprehensive plasma instrumentation, including a much expanded energy range and energy resolution compared to LP, may help us resolve some of these questions. A surface plasma/fields/dust package could also shed light on these issues.

4. Crustal magnetic anomaly interactions

The lunar crustal magnetic anomalies provide perhaps the most unique aspect of the Moon–plasma interaction. The Moon has small-scale crustal magnetic fields, with scale sizes ranging from less than one km to perhaps hundreds of km, and surface field strengths ranging from a few nT to perhaps a thousand nT, falling off rapidly with altitude to a maximum of a few tens of nT at ~30 km, and a few nT at ~100 km (Dyal et al., 1974; Halekas et al., 2001; Hood et al., 2001; Mitchell et al., 2008; Purucker, 2008). Many of the anomalies have field strengths sufficient to stand off the solar wind, but given their small scale, the pressure balance point for even the strongest anomalies should lie no more than ~20 km above the surface. Given typical proton inertial lengths and gyroradii in the solar wind on the order of ~100 km, these small vertical and lateral scales seemingly make a large-scale fluid interaction with the incoming solar wind plasma quite unlikely. Despite these basic considerations, the latest data from Kaguya and Chandrayaan strongly imply that at least some lunar crustal magnetic sources can generate a "mini-magnetosphere" capable of more or less completely shielding the surface under them from the solar wind (Saito et al., in press; Wieser et al., 2010). Indeed, it now appears that the lunar crustal magnetic sources may form the smallest magnetospheres in the solar system, if not the smallest magnetospheres physically achievable in our solar system.

The first observations of solar wind interaction with crustal magnetic anomalies came in the form of unexpected magnetic field enhancements, often seen just outside of the wake rarefaction region. Early theories for their formation included conductivity anomalies (Holweg, 1970) and atmospheric interactions (Siscoe and Mukherjee, 1972), but to date, the association with crustal magnetic fields has proven ironclad (Sonett and Mihalov, 1972; Russell and Lichtenstein, 1975; Halekas et al., 2006a),

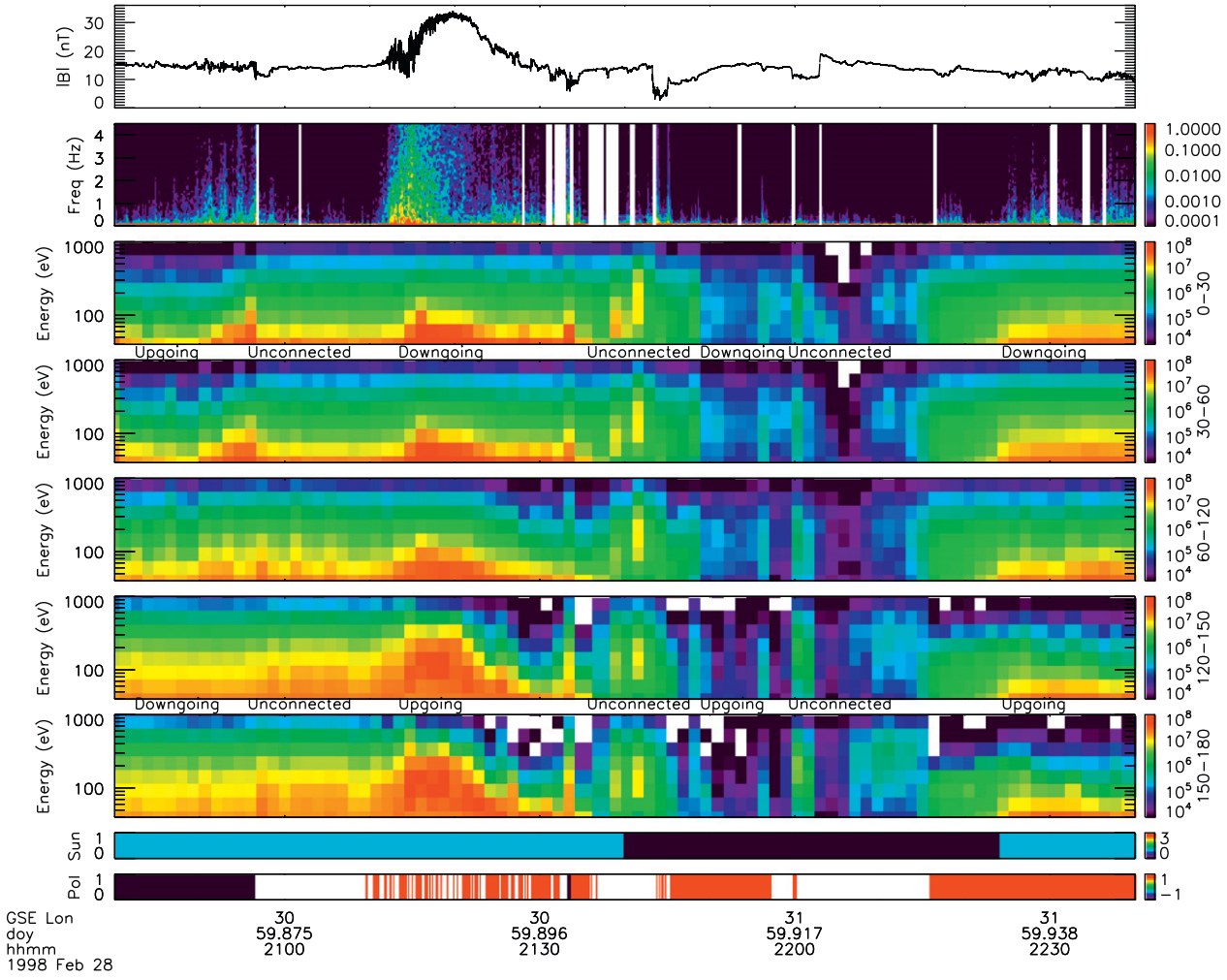

Fig. 6. Part of a Lunar Prospector orbit in the solar wind over the strong magnetic anomaly antipodal to the Imbrium basin, showing magnetic field magnitude, FFT spectrum of magnetic field fluctuations, electron differential energy flux (eV/(cm^2 sr s eV)) in five different pitch angle bins (0–30, 30–60, 60–120, 120–150, 150–180), sun/shadow color bar "Sun" (blue=sun, black=shadow), and approximate magnetic connection to surface "Pol" (assuming no field curvature, red=positive connection, black=negative connection, white=no connection). (For interpretation of the references to color in this figure legend, the reader is referred to the web version of this article.)

suggesting that these magnetic enhancements instead represent plasma compressions and/or shocks formed by solar wind interaction with crustal fields, and extending downstream from their source. Some observations argue particularly for the presence of a shock-like interaction, including density increases correlated with the field increases (Siscoe et al., 1969; Halekas et al., 2008a), and magnetic enhancements that extend significantly upstream from their apparent sources (Lin et al., 1998; Halekas et al., 2006a; Kurata et al., 2005), inconsistent with a compressional feature advected downstream with the solar wind (i.e., a magnetosonic wake).

We show a sample flyby of a typical example of such a feature, in the solar wind, over a large concentration of crustal anomalies on the lunar far side, in Fig. 6. At ~21:15–21:30, LP observes a strong magnetic enhancement, at an altitude of ~100 km. The ~30 nT peak field represents an amplification factor of ~2 over the IMF strength, and exceeds the uncompressed crustal field at orbital altitude by an order of magnitude. Thus, we can only plausibly identify this field as compressed/shocked solar wind field piled up over the anomaly; however, we find the degree of field compression surprising, given that it occurs at an altitude far above the expected pressure balance obstacle. We also see significant magnetic turbulence (second panel of Fig. 6) just upstream of the magnetic enhancement, and earlier in the orbit when magnetically connected to the surface before ~20:56. This turbulence, broadband rather than monochromatic in nature like the waves observed upstream from some interaction regions (Halekas et al., 2006b), may result from particle reflection from the surface and the resulting wave-particle instabilities (Nakagawa et al., 2009). Upstream of a crustal anomaly and/or shock-like feature such as the one observed here, one expects such reflection-generated instabilities to increase in efficiency due to increased particle reflection, consistent with the observation.

Meanwhile, during the period of maximum field compression, electron flux increases up to a few hundred eV at all angles (spectrograms in Fig. 6), implying both compression and heating, with some signs of more compression in the downward-going electron population (low energy flux enhancement) and more heating in the upward-going population (higher energy flux enhancement). During both periods of wave turbulence noted above, we observe increased electron flux coming from the surface (field-aligned flux in top spectrograms of Fig. 6 from 20:50 to 20:56, anti-field-aligned flux in bottom spectrograms of Fig. 6 from 21:10 to 21:30). Given the high degree of near-surface magnetic curvature likely near such a strong source, a straight-line trace provides only a rough approximation of the magnetic field line foot points, so we may or may not achieve surface connection, especially during the latter time period. Therefore, the increased upward-going flux could result from surface-emitted electrons accelerated by surface electrostatic fields, or by electron heating/acceleration in the crustal magnetic field interaction region. Possibly, ions penetrate deeper into the anomaly (due to their larger gyroradius and higher momentum), setting up an electric field that slows ions and accelerates electrons out of the interaction region, with this interaction also generating heating and turbulence, as previously observed by surface experiments (Clay et al., 1975; Neugebauer et al., 1972). However, the source population of such electrons, and the role of wave–particle interactions, remains unknown.

Finally, we observe bursty enhancements in electron flux at ~21:40 and 22:00 in Fig. 6, near the edge of the wake and in the center of the wake. Though not very strongly field-aligned, we suggest that these may represent electrons accelerated along magnetic field lines into a lower density region by the entry of scattered and re-picked up protons, as observed by Nishino et al. (2009b). In this case, the protons may have reflected, not from the surface, but from the anomaly interaction region.

All of the effects shown in Fig. 6 speak to the presence of a surprisingly strong and (at least in the main interaction region) coherent interaction between the solar wind and crustal magnetic anomalies, which we have yet to reconcile with theory and modeling. Simulation has provided some basic expectations for solar wind interaction with small-scale crustal anomalies. Omidi et al. (2002) modeled the solar wind interaction with dipoles with a range of strengths, finding that, as dipole strength increases, the interaction ranges from a whistler wake, to a magnetosonic wake, to a shock-like interaction, to a magnetosphere-like interaction. These models would predict at most a magnetosonic wake for the weak lunar magnetic sources. However, as Harnett and Winglee (2003) have shown, the complicated non-dipolar nature of lunar crustal anomalies may enhance the efficiency of the interaction with the solar wind. In addition, a full accounting of surface effects, including surface charging, proton reflection, electron emission, etc. may change the picture dramatically.

Until recently, we had only indirect evidence for the existence of magnetosphere-like structures above lunar crustal fields, since we only observed the shock-like enhanced magnetic fields. One might expect to find a magnetospheric cavity below these enhancements, but it could lie below the altitude of most observations. During the LP mission, only once did we observe anything like a magnetospheric cavity, at very low altitudes over the Crisium antipode (Halekas et al., 2008a). LP made this observation on a day with very unusual solar wind conditions (very high density, very low temperature, velocity and IMF strength), consistent with previous indications that solar wind conditions strongly affect the probability of formation of a magnetic enhancement (Halekas et al., 2006a) and/or the mode of interaction between the solar wind and the magnetic anomaly (Halekas et al., 2008b). Interestingly, some theoretical work suggests a stronger interaction for low Mach number (Borisov and Mall, 2003), but the LP observation instead occurred during a time period with very high Mach number.

More certain evidence for a magnetospheric cavity came only very recently, with Kaguya and Chandrayaan. Kaguya found decelerated and reflected solar wind ions over strong crustal magnetic sources, with an absence of scattered ions from the surface suggesting magnetic shielding of the surface from the solar wind (Saito et al., in press). Chandrayaan, meanwhile, similarly observed a dearth of reflected neutralized solar wind hydrogen from the surface, likewise implying magnetic shielding from the solar wind (Wieser et al., 2010). Intriguingly, the latter observation came over the same region as the LP observation described in the previous paragraph.

Further (though indirect) evidence of surface shielding may come from observations of "swirl" albedo markings on the lunar surface, with an extremely strong correlation found between these markings and strong crustal magnetic sources. These albedo markings could result either from shielding of the surface from solar wind weathering (Hood and Schubert, 1980) or (as recently suggested) from enhanced dust transport caused by electric fields in the anomaly interaction region near the surface (Garrick-Bethell et al., 2010). Either of these proposed mechanisms could have significant geologic implications, adding yet another reason to study the fundamental physical properties of the solar wind interaction with crustal magnetic sources.

5. The lunar plasma physics laboratory

The Moon provides us with a natural plasma physics laboratory – right in our back yard, cosmically speaking. The lunar environment gives us a natural place to investigate fundamental plasma physics and related phenomena that operate throughout the solar system, such as surface charging, wake

formation, exospheric source and loss processes, surface weathering, etc. The Moon also gives us a wonderful laboratory in which to study kinetic phenomena, given the small scales of many of the interaction regions as compared to relevant plasma scales. Finally, the Moon unquestionably provides a unique environment for studying plasma instabilities and wave–particle interactions, with applicability throughout the solar system.

At the Moon, we can study a variety of foreshock-like processes, including wave turbulence upstream from dayside regions with (Halekas et al., 2006b) and without (Nakagawa et al., 2009) magnetic anomalies, and on magnetic field lines connected to the wake (Nakagawa et al., 2009; Farrell et al., 1996). These waves, ranging from monochromatic whistlers to broad-spectrum turbulence, may variously result from charged particle reflection from the surface, crustal fields and wake boundary, and charged particle filtration and acceleration by electrostatic fields in the wake and magnetic anomaly interaction regions. A number of other processes, meanwhile, may produce waves by generating unstable (non-Maxwellian) distribution functions and/or beam–beam instabilities. For example, solar wind protons that bi-directionally refill the wake along field lines may produce electrostatic turbulence (Farrell et al., 1998) and electron phase space holes (Birch and Chapman, 2001a, 2001b). Electrons pulled into the wake along magnetic field lines by charge imbalances from Type-II entry of re-picked up solar wind ions unquestionably produce electrostatic turbulence (Nishino et al., in press). Pickup ions themselves likely produce unstable distributions, as does the electrostatic filtration effect of the wake (imagine for instance, a case where the wake ambipolar field excludes the entire electron core, leaving only a strongly beamed strahl population, part of which could also reflect and produce a counter-streaming distribution). Finally, the Moon provides a source of particles that can affect the plasma environment around it, including reflected protons, sputtered ions, ionized exospheric constituents, photoelectrons from the surface, and secondary electrons produced by electron and ion impact, etc. Any and all of these source processes can and likely to produce particle distributions unstable to wave growth.

In addition, the Moon provides a unique environment in which to study processes where ions and electrons decouple from each other; for instance, the thin plasma interface at the surface, the wake boundary region, and the tiny crustal magnetic anomaly interaction regions. We can investigate fundamental plasma processes in these regions that may prove relevant for our understanding of shocks and other plasma discontinuities, and perhaps even reconnection. The Moon could prove particularly convenient for such studies, since we can easily locate the region of interest, rather than searching a large and highly variable region for other examples of these phenomena.

Many fundamental lunar plasma processes will also operate at other airless bodies throughout the solar system (e.g. Mercury, outer planet moons, asteroids, KBOs, etc.) – probably in similar fashion to how they operate at the Moon. Additionally, many of these same processes also work in completely different environments, like magnetized planets and moons (e.g., Ganymede, the giant planets, etc.), un-magnetized planets with atmospheres (e.g. Mars, Venus, Titan, etc.). Even in the tenuous lunar environment, most lunar plasma processes can act in concert and couple to each other; however, some processes may couple only weakly compared to other planetary environments. In that case, the Moon provides an opportunity to explore fundamental physics in a regime where processes do not couple as strongly as they will in a more complicated plasma environment. Thus, the Moon represents both a keystone for the study of airless bodies, and a test bed for the study of plasma processes throughout the solar system and beyond.

6. The future

In many respects, it may seem that we have learned much of what there is to know about the lunar plasma environment. However, in truth, we still know very little about many fundamental aspects of the Moon–plasma interaction, and how it affects (and is affected by) other aspects of the lunar environment. We have discussed some of these problems in detail in this paper, and commented extensively on the remaining work that must be done. Truly fascinating science remains before we understand the full picture of the surface interaction, the wake, or the interaction with crustal magnetic fields.

A satisfactory description of crustal field interactions may require a fundamentally new paradigm in order to understand how the solar wind interacts so efficiently with such small-scale features. We still need to understand whether this interaction represents a bow shock and magnetosphere as we typically understand the terms, or whether our observations actually indicate something rather different. We also have far to go before we can relate the small-scale microphysics of the interaction to the global-scale features. We have not even begun the difficult task of determining the importance of surface effects on the plasma-magnetic anomaly interaction, and in turn, the effects of the interaction on the surface.

Speaking of the surface, we clearly have much to learn about the details of the plasma-surface interface. Our understanding of single particle interactions with the surface remains rudimentary. We know that solar wind particles cause sputtering, produce components of the exosphere and pickup ions, generate secondary particles, and charge the surface. However, we do not yet fully understand the detailed chemistry of these interactions. For instance, solar wind implanted hydrogen may have some connection to the significant stores of water and other molecules on the Moon recently discovered by LCROSS (Colaprete et al., 2010), as proposed by Vondrak and Crider (2003) and others. Also, a solar wind/regolith chemical process has been specifically mentioned as a possible source of the 3-micron absorption feature (identifying water/hydroxyl) recently observed by Chandrayaan, Deep Impact, and Cassini (Pieters et al., 2010; Sunshine et al., 2009; Clark, 2009). Conversely, proton impact on an already ice-rich surface, which has a high sputtering yield, could effectively erode ice and remove any water build-up (Farrell et al., 2010). Thus, plasma impact could potentially affect both the source and loss processes for lunar ice deposits.

In general, we have much to learn about the interactions between plasma and other components of the lunar environment. How does the surface chemistry produced by plasma impact affect the geology of the near surface? To what degree does plasma impact act to weather surfaces? Can magnetic shielding from plasma impact account for lunar albedo swirls? How does the electrostatic environment around the Moon affect dust, and how much, in turn, does charged dust affect the plasma environment around it? How much of the exosphere does charged particle impact generate, and how does the ionized component of that exosphere feed back into the plasma environment? These and more fundamental questions, with relevance to all areas of lunar science, await solution.

We are not done with lunar plasma science, or with lunar science in general. Luckily, huge volumes of data from previous and current missions await analysis, as does data from future missions like ARTEMIS and LADEE. The path forward seems clear in many regards, but we should have no doubt that the most interesting discoveries awaiting us, as always, will prove to be the inevitable unexpected and serendipitous finds that have come every time a new mission with new instrumentation has visited the Moon.

Acknowledgements

We thank NASA's Lunar Science Institute for supporting this work.

References

Alvarez, R. 1977. Photoconductive effects on lunar and terrestrial fines. In: Proceedings of the 8th Lunar Science Conference, pp. 1277–1290.

Anderson, K.A., Lin, R.P., McGuire, R.E., McCoy, J.E., 1975. Measurement of lunar and planetary magnetic fields by reflection of low energy electrons. Space Sci. Inst. 1, 439–470.

Angelopoulos, V., Lillis, R., Sibeck, D.G., Halekas, J., Delory, G.T., Khurana, K.K., Russell, C.T., McFadden, J.P., Bonnell, J., Larson, D., 2010. ARTEMIS, a two spacecraft, planetary and heliospheric lunar mission. In: 41st Lunar and Planetary Science Conference, p. 1425.

Bale, S.D., Owen, C.J., Bougeret, J.-L., Goetz, K., Kellogg, P.J., Lin, R.P., Manning, R., Monson, S.J., 1997. Evidence of currents and unstable particle distributions in an extended region around the lunar wake. Geophys. Res. Lett. 24, 1427–1430.

Benson, J., 1977. Direct measurements of the plasma screening length and surface potential near the lunar terminator. J. Geophys. Res. 82 (13), 1917–1920.

Berg, O.E., Wolf, H., Rhee, J.W., 1976. Lunar soil movement registered by the Apollo 17 cosmic dust experiment. In: Elsässer, H., Fechtig, H. (Eds.), Interplanetary Dust and Zodiacal Light. Springer-Verlag, Berlin, pp. 233–237.

Birch, P.C., Chapman, S.C., 2001a. Particle-in-cell simulations of the lunar wake with high phase space resolution. Geophys. Res. Lett. 28, 219.

Birch, P.C., Chapman, S.C., 2001b. Detailed structure and dynamics in particle-in-cell simulations of the lunar wake. Phys. Plasmas 8, 4551–4559.

Borisov, N., Mall, U., 2003. Interaction of the solar wind with a localized magnetic barrier: application to lunar surface magnetic fields. Phys. Lett. A 309, 277–289.

Borisov, N., Mall, U., 2006. Charging and motion of dust grains near the terminator of the moon. Planet. Space Sci. 54, 572–580.

Clack, D., Kasper, J.C., Lazarus, A.J., Steinberg, J.T., Farrell, W.M., 2004. Wind observations of extreme ion temperature anisotropies in the lunar wake. Geophys. Res. Lett. 31, L06812. doi:10.1029/2003GL018298.

Cladis, J.B., Francis, W.E., Vondrak, R.R., 1994. Transport towards Earth of ions sputtered from the Moon's surface by the solar wind. J. Geophys. Res. 99 (A1), 53–64.

Clark, R.N., 2009. Detection of Adsorbed Water and Hydroxyl on the Moon. Science 326, 562.

Clay, D.R., Goldstein, B.E., Neugebauer, M., Snyder, C.W., 1975. Lunar surface solar wind observations at the Apollo 12 and Apollo 15 sites. J. Geophys. Res. 80, 1751–1760.

Colaprete, A., Ennico, K., Wooden. D., Shirley, M., Heldmann, J., Marshall, W., Sollitt, L., Asphaug, E., Korycansky, D., Shultz, P., Hermalyn, B., Galal, K., Bart, G.D., Goldstein, D., Summy, D., 2010. Water and more: an overview of LCROSS impact results. In: 41st Lunar Planetary Science Conference, p. 2335.

Colburn, D.S., Mihalov, J.D., Sonett, C.P., 1971. Magnetic observations of the lunar cavity. J. Geophys. Res. 76, 2940–2957.

Colburn, D.S., Currie, R.G., Mihalov, J.D., Sonett, C.P., 1967. Diamagnetic solar-wind cavity discovered behind moon. Science 158, 1040.

Coleman, P.J., Lichtenstein, B.R., Russell, C.T., Sharp, L.R., Schubert, G., 1972. Magnetic fields near the Moon. Geochem. Cosmochem. Acta 36, 2271–2286.

Colwell, J.E., Robertson, S.R., Horányi, M., Wang, X., Poppe, A., Wheeler, P., 2009. Lunar dust levitation. J. Aerospace Eng. 22, 2–9.

Criswell, D.R., De, B.R., 1977. Intense localized charging in the lunar sunset terminator region. 2. Supercharging at the progression of sunset. J. Geophys. Res. 82, 1005–1007.

Crow, J.E., Auer, P.L., Allen, J.E., 1975. The expansion of plasma into a vacuum. J. Plasma Phys. 14, 65–76.

De, B.R., Criswell, D.R., 1977. Intense localized photoelectric charging in the lunar sunset terminator region. 1. Development of potentials and fields. J. Geophys. Res. 82, 999–1004.

Denavit, J., 1979. Collisionless plasma expansion into a vacuum. Phys. Fluids 22, 1384–1392.

Doe, S.J., Burns, O., Pettit, D., Blacic, J., Keaton, P.W., 1994. The levitation of lunar dust via electrostatic forces, in Engineering, Construction, and Operations in Space. Am. Soc. Civil Eng., New York, pp. 907–915.

Dolginov, S.S., Yeroshenko, Y.G., Zhuzgov, L.N., Pushkov, N.V., Tyurmina, L.O., 1960. Measuring the magnetic fields of the earth and moon by means of Sputnik 3 and space rockets 1 and 2. Space Res. 1, 863–868.

Dyal, P., Parkin, C.W., Daily, W.D., 1974. Magnetism and the interior of the Moon. Rev. Geophys. Space Phys. 12, 568–591.

Elphic, R.C., Funsten III, H.O., Barraclough, B.L., McComas, D.J., Paffett, M.T., Vaniman, D.T., Heiken, G., 1991. Lunar surface composition and solar wind-induced secondary ion mass spectrometry. Geophys. Res. Lett. 18, 2165.

Farrell, W.M., Fitzenreiter, R.J., Owen, C.J., Byrnes, J.B., Lepping, R.P., Ogilvie, K.W., Neubauer, F., 1996. Upstream ULF waves and energetic electrons associated with the lunar wake: detection of precursor activity. Geophys. Res. Lett. 23, 1271–1274.

Farrell, W.M., Kaiser, M.L., Steinberg, J.T., Bale, S.D., 1998. A simple simulation of a plasma void: applications to wind observations of the lunar wake. J. Geophys. Res. 103, 23653–23660.

Farrell, W.M., Stubbs, T.J., Halekas, J.S., Delory, G.T., Collier, M.R., Vondrak, R.R., Lin, R.P., 2008a. Loss of solar wind plasma neutrality near the lunar terminator and polar regions. Geophys. Res. Lett. 35, L015105. doi:10.1029/2007GL032653.

Farrell, W.M., Stubbs, T.J., Delory, G.T., Vondrak, R.R., Collier, M.R., Halekas, J.S., Lin, R.P., 2008b. Concerning the dissipation of electrically charged objects in the shadowed lunar polar regions. Geophys. Res. Lett. 35, L19104. doi:10.1029/2008GL04785.

Farrell, W.M., Stubbs, T.J., Halekas, J.S., Killen, R.M., Delory, G.T., Collier, M.R., Vondrak, R.R., 2010. Anticipated electrical environment within permanently shadowed lunar craters. J. Geophys. Res 115, E03004. doi:10.1029/2009JE003464.

Fenner, M.A., Freeman, J.W., Hills, H.K., 1973. The electric potential of the lunar surface. In: Proceedings of the 4th Lunar Science Conference, vol. 3, pp. 2877–2887.

Freeman, J.W., Ibrahim, M., 1975. Lunar electric fields, surface potential and associated plasma sheaths. Moon 14, 103–114.

Freeman Jr., J.W., Fenner, M.A., Hills, H.K., 1973. Electric potential of the Moon in the solar wind. J. Geophys. Res. 78, 4560–4567.

Freeman Jr., J.W., Fenner, M.A., Hills, H.K., Lindeman, R.A., Medrano, R., Meister, J., 1972. Suprathermal ions near the moon. Icarus 16, 328–338.

Fu, J.H.M., 1971. Surface potential of a photoemitting plate. J. Geophys. Res. 76, 2506–2509.

Futaana, Y., Machida, S., Saito, Y., Matsuoka, A., Hayakawa, H., 2001. Counter-streaming electrons in the near vicinity of the Moon observed by plasma instruments on board NOZOMI. J. Geophys. Res. 106, 18729–28740.

Futaana, Y., Machida, S., Saito, Y., Matsuoka, A., Hayakawa, H., 2003. Moon-related nonthermal ions observed by Nozomi: species, sources, and acceleration mechanisms. J. Geophys. Res., 108. doi:10.1029/2002JA009366.

Garrick-Bethell, I., Head, J.W. III, Pieters, C.M., 2010. Spectral properties of lunar swirls and their formation by dust transport. In: 41st Lunar Planetary Science Conference, p. 2675.

Guernsey, R.L., Fu, J.H.M., 1970. Potential distribution surrounding a photo-emitting plate in a dilute plasma. J. Geophys. Res. 75 (16), 3193–3199.

Halekas, J.S., Mitchell, D.L., Lin, R.P., Frey, S., Hood, L.L., Acuña, M.H., Binder, A.B., 2001. Mapping of crustal magnetic anomalies on the lunar near side by the Lunar Prospector electron reflectometer. J. Geophys. Res. 106, 27841–27852.

Halekas, J.S., Mitchell, D.L., Lin, R.P., Hood, L.L., Acuña, M.H., 2002. Evidence for negative charging of the lunar surface in shadow. Geophys. Res. Lett., 29. doi:10.1029/2001GL014428.

Halekas, J.S., Lin, R.P., Mitchell, D.L., 2003. Inferring the scale height of the lunar nightside double layer. Geophys. Res. Lett., 30. doi:10.1029/2003GL018421.

Halekas, J.S., Lin, R.P., Mitchell, D.L., 2005a. Large negative lunar surface potentials in sunlight and shadow. Geophys. Res. Lett. 32, L09102. doi:10.1029/2005GL022627.

Halekas, J.S., Bale, S.D., Mitchell, D.L., Lin, R.P., 2005b. Magnetic fields and electrons in the lunar plasma wake. J. Geophys. Res. 110, A07222. doi:10.1029/2004JA010991.

Halekas, J.S., Brain, D.A., Mitchell, D.L., Lin, R.P., Harrison, L., 2006a. On the occurrence of magnetic enhancements caused by solar wind interaction with lunar crustal fields. Geophys. Res. Lett. 33, L01201. doi:10.1029/2006GL025931.

Halekas, J.S., Brain, D.A., Mitchell, D.L., Lin, R.P., 2006b. Whistler waves observed near lunar crustal magnetic sources. Geophys. Res. Lett. 33, L22104. doi:10.1029/2006GL027684.

Halekas, J.S., Delory, G.T., Brain, D.A., Lin, R.P., Fillingim, M.O., Lee, C.O., Mewaldt, R.A., Stubbs, T.J., Farrell, W.M., Hudson, M.K., 2007. Extreme lunar surface charging during solar energetic particle events. Geophys. Res. Lett. 34, L02111. doi:10.1029/2006GL028517.

Halekas, J.S., Delory, G.T., Brain, D.A., Lin, R.P., Mitchell, D.L., 2008a. Density cavity observed over a strong lunar crustal magnetic anomaly in the solar wind: a mini-magnetosphere? Planet. Space Sci. 56/ 7, 941–946. doi:10.1016/j.pss.2008.01.008.

Halekas, J.S., Brain, D.A., Lin, R.P., Mitchell, D.L., 2008b. Solar wind interaction with lunar crustal magnetic anomalies. J. Adv. Space Res. 41, 1319–1324. doi:10.1016/j.asr.2007.04.003.

Halekas, J.S., Delory, G.T., Lin, R.P., Stubbs, T.J., Farrell, W.M., 2008c. Lunar Prospector observations of the electrostatic potential of the lunar surface and its response to incident currents. J. Geophys. Res. 113, A09102. doi:10.1029/2008JA013194.

Halekas, J.S., Delory, G.T., Lin, R.P., Stubbs, T.J., Farrell, W.M., 2009a. Lunar Prospector measurements of secondary electron emission from lunar regolith. Planet. Space. Sci. 57, 78–82. doi:10.1016/j.pss.2008.11.2009.

Halekas, J.S., Delory, G.T., Lin, R.P., Stubbs, T.J., Farrell, W.M., 2009b. Lunar surface charging during solar energetic particle events: measurement and prediction. J. Geophys. Res. 114, A05110. doi:10.1029/2009JA014113.

Halekas, J.S., Lillis, R.J., Lin, R.P., Manga, M., Purucker, M.E., Carley, R.A., 2010. How strong are lunar crustal magnetic fields at the surface: considerations from a reexamination of the electron reflectometry technique. J. Geophys. Res. 115, E03006. doi:10.1029/2009JE003516.

Harnett, E.M., Winglee, R., 2003. 2.5-D simulations of the solar wind interacting with multiple dipoles on the surface of the Moon. J. Geophys. Res. 109, 1088. doi:10.1029/2002JA009617.

Hartle, R.E., Killen, R., 2006. Measuring pickup ions to characterize the surfaces and exospheres of planetary bodies: applications to the Moon. Geophys. Res. Lett. 33, L05201. doi:10.1029/2005GL024520.

Hilchenbach, M., Hovestadt, D., Klecker, B., Mobius, E., 1993. Observation of energetic lunar pick-up ions near Earth. Adv. Space Res. 13 (10), 321–324.
Hoffman, J.H., Hodges R.R. Jr., Evans D.E., 1973. Lunar atmospheric composition results from Apollo 17. In: Proceedings of the 4th Lunar Science Conference, p. 2875.
Hollweg, J.V., 1970. Lunar conducting islands and formation of a lunar limb shock wave. J. Geophys. Res. 75, 1209–1216.
Holmström, M., Weiser, M., Barabash, S., Futaana, Y., Bhardwaj, A., in press. Dynamics of solar wind protons reflected by the Moon, J. Geophys. Res., doi:10.1029/2009JA014843.
Hood, L.L., Schubert, G., 1980. Lunar magnetic anomalies and surface optical properties. Science 208, 49–51.
Hood, L.L., Zakharian, A., Halekas, J., Mitchell, D.L., Lin, R.P., Acuña, M.H., Binder, A.B., 2001. Initial mapping and interpretation of lunar crustal magnetic anomalies using Lunar Prospector magnetometer data. J. Geophys. Res. 106, 27,825–27,840.
Horányi, M., 1996. Charged dust dynamics in the solar system. Annu. Rev. Astron. Astrophysics 34, 383–418.
Johnson, F., Midgeley, J.E., 1968. Notes on the lunar magnetosphere. J. Geophys. Res. 73, 1523.
Kallio, E., 2005. Formation of the lunar wake in quasi-neutral hybrid model. Geophys. Res. Lett. 32, L06107. doi:10.1029/2004GL021989.
Kimura, S., Nakagawa, T., 2008. Electromagnetic full particle simulation of the electric field structure around the moon and the lunar wake. Earth Planet. Space 60, 591–599.
Kurata, M., Tsunakawa, H., Saito, Y., Shibuya, H., Matsushima, M., Shimizu, H., 2005. Mini-magnetosphere over the Reiner Gamma magnetic anomaly region on the Moon. Geophys. Res. Lett. 32, L24205. doi:10.1029/2005GL024097.
Lin, R.P., Mitchell, D.L., Curtis, D.W., Anderson, K.A., Carlson, C.W., McFadden, J., Acuña, M.H., Hood, L.L., Binder, A., 1998. Lunar surface magnetic fields and their interaction with the solar wind: results from Lunar Prospector. Science 281, 1480–1484.
Lindeman, R., Freeman, J.W., Vondrak, R.R., 1973. Ions from the lunar atmosphere. In: Proceedings of the 4th Lunar Science Conference, pp. 2889–2896.
Mall, U., Kirsch, E., Cierpka, K., Wilken, B., Söding, A., Neubauer, F., Gloeckler, G., Galvin, A., 1998. Direct observation of lunar pick-up ions near the Moon. Geophys. Res. Lett. 25 (20), 3799–3802.
Manka, R.H., 1973. Plasma and potential at the lunar surface. In: Grard, R.J.L., Reidel, D. (Eds.), Photon and Particle Interactions with Surfaces in Space, pp. 347–361.
McComas, D.J., Allegrini, F., Bochsler, P., Frisch, P., Funsten, H.O., Gruntman, M., Janzen, P.H., Kucharek, H., Möbius, E., Reisenfeld, D.B., Schwadron, N.A., 2009. Lunar backscatter and neutralization of the solar wind: first observations of neutral atoms from the Moon. Geophys. Res. Lett. 36, L12104. doi:10.1029/2009GL038794.
McCoy, J.E., Criswell, D.R., 1974. Evidence for a high altitude distribution of lunar dust. Proc. Lunar Sci. Conf. 5, 2991–3005.
Michel, F.C., 1968. Magnetic field structure behind the Moon. J. Geophys. Res. 73, 1533–1541.
Mitchell, D.L., Halekas, J.S., Lin, R.P., Frey, S., Hood, L.L., Acuna, M.H., Binder, A., 2008. Global mapping of lunar crustal magnetic fields by Lunar Prospector. Icarus 194, 401–409. doi:10.1016/j.icarus.2007.10.027.
Nakagawa, T., Iizima, M., 2006. A reexamination of pitch angle diffusion of electrons at the boundary of the lunar wake. Earth Planets Space 58, e17–e20.
Nakagawa, T., Takahashi, Y., Iizima, M., 2003. GEOTAIL observation of upstream ULF waves associated with the lunar wake. Earth Planets Space 55, 569–580.
Nakagawa, T., Takahashi, F., Tsunakawa, H., Shibuya, H., Shimizu, H., Matsushima, M., 2009. Non-monochromatic whistler waves detected by Kaguya on the dayside surface of the moon. Earth Planet. Space, 61.
Ness, N.F., 1972. Interaction of the solar wind with the Moon. In: Dyer (Ed.), Solar Terrestrial Physics/1970, Part II. D. Reidel Publ. Comp., Dordrecht, pp. 159–205.
Ness, N.F., Behannon, K.W., Taylor, H.E., Whang, Y.C., 1968. Perturbations of the interplanetary magnetic field by the lunar wake. J. Geophys. Res. 73, 3421–3440.
Ness, N.F., Behannon, K.W., Searce, C.S., Cantarano, S.C., 1967. Early results from the magnetic field instrument on lunar Explorer 35. J. Geophys. Res. 72, 5769–5778.
Neugebauer, M., Snyder, C.W., Clay, D.R., Goldstein, B.E., 1972. Solar wind observations on the lunar surface with the Apollo 12 ALSEP. Planet. Space Sci. 20, 1577–1591.
Nitter, T., Havnes, O., 1992. Dynamics of dust in a plasma sheath and injection of dust into the plasma sheath above moon and asteroidal surfaces. Earth Moon Planet 56, 7–34.
Nitter, T., Havnes, O., Melandsø, F., 1998. Levitation and dynamics of charged dust in the photoelectron sheath above surfaces in space. J. Geophys. Res. 103, 6605–6620.
Nishino, M.N., Maezawa, K., Fujimoto, M., Saito, Y., Yokota, S., Asamura, K., Tanaka, T., Tsunakawa, H., Matsushima, M., Takahashi, F., Terasawa, T., Shibuya, H., Shimizu, H., 2009a. Pairwise energy gain-loss feature of solar wind protons in the near-Moon wake. Geophys. Res. Lett. 36, L12108. doi:10.1029/2009GL039049.
Nishino, M.N., Fujimoto, M., Maezawa, K., Saito, Y., Yokota, S., Asamura, K., Tanaka, T., Tsunakawa, H., Matsushima, M., Takahashi, F., Terasawa, T., Shibuya, H., Shimizu, H., 2009b. Solar-wind proton access deep into the near-Moon wake. Geophys. Res. Lett. 36, L16103. doi:10.1029/2009GL039444.
Nishino, M.N., Fujimoto, M., Saito, Y., Yokota, S., Y., Kasahara, Omura, Y., Goto, Y., Hashimoto, K., Kumamoto, A., Ono, T., Tsunakawa, H., Matsushima, M., Takahashi, F., Shibuya, H., Shimizu, H., Terasawa, T., in press. Effect of the solar wind proton entry into the deepest lunar wake. Geophys. Res. Lett., 37, doi:10.1029/2010GL042607.
Ogilvie, K.W., Steinberg, J.T., Fitzenreiter, R.J., Owen, C.J., Lazarus, A.J., Farrell, W.M., Torbert, R.B., 1996. Observations of the lunar plasma wake from the WIND spacecraft on December 27, 1994. Geophys. Res. Lett. 10, 1255–1258.
Omidi, N., Blanco-Cano, X., Russell, C.T., Karimabadi, H., Acuña, M., 2002. Hybrid simulations of solar wind interaction with magnetized asteroids: general characteristics. J. Geophys. Res. 107, 1487. doi:10.1029/2002JA009441.
Owen, C.J., Lepping, R.P., Ogilvie, K.W., Slavin, J.A., Farrell, W.M., Byrnes, J.B., 1996. The lunar wake at 6.8 R_L: WIND magnetic field observations. Geophys. Res. Lett. 10, 1263–1266.
Pieters, C.M., Goswami, J.N., Clark, R.N., Annadurai, M., Boardman, J., Buratti, B., Combe, J.-P., Dyar, M.D., Green, R., Head, J.W., Hibbitts, C., Hicks, M., Isaacson, P., Klima, R., Kramer, G., Kumar, S., Livo, E., Lundeen, S., Malaret, E., McCord, T., Mustard, J., Nettles, J., Petro, N., Runyon, C., Staid, M., Sunshine, J., Taylor, L.A., Tompkins, S., Varanasi, P., 2010. Character and spatial distribution of OH/H_2O on the surface of the Moon seen by M^3 on Chandrayaan. Science 326, 568–572.
Poppe, A., Horányi, M., in review, Simulations of the photoelectron sheath and dust levitation on the lunar surface. J. Geophys. Res.
Purucker, M.E., 2008. A global model of the internal magnetic field of the Moon based on Lunar Prospector magnetometer observations. Icarus 197, 19–23. doi:10.1016/j.icarus.2008.03.016.
Reasoner, D.L., Burke, W.J., 1972. Characteristics of the lunar photoelectron layer in the geomagnetic tail. J. Geophys. Res. 77, 6671–6687.
Rennilson, J.J., Criswell, D.R., 1974. Surveyor observations of lunar horizon-glow. Moon 10, 121–142.
Russell, C.T., Lichtenstein, B.R., 1975. On the source of lunar limb compression. J. Geophys. Res. 80, 4700.
Russell, C.T., Coleman, P.J., Schubert, G., 1978. The permanent and induced dipole moment of the Moon. Lunar Planetary Science Conference 5, 2747.
Saito, Y., Yokota, S., Tanaka, T., Asamura, K., Nishino, M.N., Fujimoto, M., Tsunakawa, H., Shibuya, H., Matsushima, M., Shimizu, H., Takahashi, F., Mukai, T., Terasawa, T., 2008. Solar wind proton reflection at the lunar surface: low energy ion measurements by MAP-PACE onboard SELENE (KAGUYA). Geophys. Res. Lett. 35, L24205. doi:10.1029/2008GL036077.
Saito, Y., Yokota, S., Asamura, K., Tanaka, T., M.N. Nishino, Yamamoto, T., Terakawa, Y., Fujimoto, M., Hasegawa, H., Hayakawa, H., Hirahara, M., Hoshino, M., Machida, S., Mukai, T., Nagai, T., Nagatsuma, T., Nakagawa, T., Nakamura, M., Oyama, K., Sagawa, E., Sasaki, S., Seki, K., Shinohara, I., T. Terasawa, Tsunakawa, H., Shibuya, H., Matsushima, M., Shimizu, H., Takahashi, F., in press. In-flight performance and initial results of Plasma energy angle and composition experiment (PACE) on SELENE (Kaguya), Space Sci. Rev.
Samir, U., Wright Jr., K.H., Stone, N.H., 1983. The expansion of a plasma into a vacuum: basic phenomena and processes and applications to space plasma physics. Rev. Geophys. 21, 1631–1646.
Schubert, G., Lichtenstein, B.R., 1974. Observations of Moon–plasma interactions by orbital and surface experiments. Rev. Geophys. 12, 592–626.
Schwerer, F.C., Huffman, G.P., Fisher, R.M., Nagata, T., 1974. Electrical conductivity of lunar surface rocks; laboratory measurements and implications for lunar interior temperatures. In: Proceedings of the 5th Lunar Science Conference, pp. 2673–2687.
Sickafoose, A.A., Colwell, J.E., Horányi, M., Robertson, S., 2002. Experimental levitation of dust grains in a plasma sheath. J. Geophys. Res. 107. doi:10.1029/2002JA009347.
Singer, S.F., Walker, E.H., 1962. Photoelectric screening of bodies in interplanetary space. Icarus 1, 7–12.
Siscoe, G.L., Mukherjee, N.R., 1972. Upper limits on the lunar atmosphere determined from solar wind measurements. J. Geophys. Res. 77, 6042.
Siscoe, G.L., Lyon, E.F., Binsach, J.H., Bridge, H.S., 1969. Experimental evidence for a detached lunar compression wave. J. Geophys. Res. 74, 59–69.
Sonett, C.P., 1982. Electromagnetic induction in the Moon. Rev. Geophys. Space Phys. 20, 411–455.
Sonett, C.P., Mihalov, J.D., 1972. Lunar fossil magnetism and perturbations of the solar wind. J. Geophys. Res. 77, 588–603.
Sonett, C.P., Colburn, D.S., Currie, R.G., 1967. The intrinsic magnetic field of the moon. J. Geophys. Res. 72, 5503.
Spreiter, J.R., Marsch, M.C., Summers, A.L., 1970. Hydromagnetic aspects of solar wind flow past the Moon. Cosmic Electrodynam 1, 5.
Stern, S.A., 1999. The lunar atmosphere: history, status, current problems, and context. Rev. Geophys 37 (4), 453–491.
Stubbs, T.E., Vondrak, R.R., Farrell, W.M., 2006. A dynamic fountain model for lunar dust. Adv. Space Res. 37 (59), 2006.
Stubbs, T.J., Vondrak, R.R., Farrell, W.M., 2007a. Impact of dust on lunar exploration. In: Krüger, H., Graps, A.L. (Eds.), Dust in Planetary Systems, Workshop, September 26–30 2005, Kauai, HI, ESA Publications, SP-643, pp. 239–244.
Stubbs, T.J., Halekas, J.S., Farrell, W.M., Vondrak, R.R., 2007b. Lunar surface charging: a global perspective using Lunar Prospector data. In: Krüger, H., Graps, A.L. (Eds.), Dust in Planetary Systems, Workshop, September 26–30 2005, Kauai, HI, ESA Publications, SP-643, pp. 181–184.
Stubbs, T.J., Vondrak, R.R., Farrell, W.M., 2007c. A dynamic fountain model for dust in the lunar exosphere. In: Krüger, H., Graps, A.L. (Eds.), Dust in Planetary

Systems, Workshop, September 26–30 2005, Kauai, HI, ESA Publications, SP-643, pp. 185–190.
Sunshine, J.M., Farnham, T.L., Feaga, L.M., Groussin, O., Merlin, F., Milliken, R.E., A'Hearn, M.F., 2009. Temporal and spatial variability of lunar hydration as observed by the deep impact spacecraft. Science 326, 565.
Tanaka, T., Saito, Y., Yokota, S., Asamura, K., Nishino, M.N., Tsunakawa, H., Shibuya, H., Matsushima, M., Shimizu, H., Takahashi, F., Fujimoto, M., Mukai, T., Terasawa, T., 2009. First in situ observation of the Moon-originating ions in the Earth's Magnetosphere by MAP-PACE on SELENE (KAGUYA). Geophys. Res. Lett. 22, L22106. doi:10.1029/2009GL040682.
Trávnicek, P., Hellinger, P., 2005. Structure of the lunar wake: two-dimensional global hybrid simulations. Geophys, Res. Lett. 32, L06102. doi:10.1029/2004GL022243.
Vondrak, R.R., Crider, D.H., 2003. Ice at the lunar poles. Am. Sci. 91, 322.
Wang, X., Horányi, M., Robertson, S., 2009. Experiments on dust transport in plasma to investigate the origin of the lunar horizon glow. J. Geophys. Res. 114, A05103. doi:10.1029/2008JA013983.
Wang, X.-D., Bian, W., Wang, J.-S., Liu, J.-J., Zou, Y.-L., Zhang, H.-B., Lü, C., Liu, J.-Z., Zuo, W., Su, Y., Wen, W.-B., Wang, M., Ouyang, Z.-Y., Li, C.-L., 2010. Acceleration of scattered solar wind protons at the polar terminator of the Moon: results from chang'E-1/SWIDs. Geophys. Res. Lett. 37, L07203. doi:10.1029/2010GL042891.
Whang, Y.C., 1968a. Interaction of the magnetized solar wind with the Moon. Phys. Fluids 11, 969–975.
Whang, Y.C., 1968b. Theoretical study of the magnetic field in the lunar wake. Phys. Fluids 11, 1713–1719.
Whang, Y.C., Ness, N.F., 1970. Observations and interpretation of the lunar Mach cone. J. Geophys. Res. 75, 6002–6010.
Wieser, M., Barabash, S., Futaana, Y., Holmstrom, M., Bhardwaj, A., Sridharan, R., Dhanya, M.B., Wurz, P., Schaufelberger, A., Asamura, K., 2009. Extremely high reflection of solar wind protons as neutral hydrogen atoms from regolith in space, Planet. Space. Sci., 10.1016/j.pss.2009.09.012.
Wieser, M., Barabash, S., Futaana, Y., Holmstrom, M., Bhardwaj, A., Sridharan, R., Dhanya, M.B., Wurz, P., Schaufelberger, A., Asamura, K., 2010. First observation of a mini-magnetosphere above a lunar magnetic anomaly using energetic neutral atoms. Geophys. Res. Lett. 37, L015103. doi:10.1029/2009GL041721.
Whipple, E.C., 1981. Potentials of surfaces in space. Rep. Prog. Phys. 44, 1197–1250.
Yokota, S., Saito, Y., Asamura, K., Tanaka, T., Nishino, M.N., Tsunakawa, H., Shibuya, H., Matsushima, M., Shimizu, H., Takahashi, F., Fujimoto, M., Mukai, T., Terasawa, T., 2009. First direct detection of ions originating from the Moon by MAP-PACE IMA onboard SELENE (KAGUYA). Geophys. Res. Lett. 36, L11201. doi:10.1029/2009GL038185.
Yokota, S., Saito, Y., 2005. Estimation of picked-up lunar ions for future compositional remote SIMS analyses of the lunar surface. Earth Planets Space 57, 281–289.
Zook, H.A., McCoy, J.E., 1991. Large scale lunar horizon glow and a high altitude lunar dust exosphere. Geophys. Res. Lett. 18, 2117–2120.